TABLE II

SUMMARY OF THE ARC MEASUREMENT RESULTS TO ESTIMATE THE ANTENNA GAIN OF PR-BBM BOTH FOR THE TRANSMISSION AND RECEPTION. THE VALUES OF ANTENNA GAIN OBTAINED FROM THE MEASUREMENT ARE COMPARED WITH THOSE OBTAINED FROM CALCULATION

Method	Measurement results regarding PR-BBM	PR-BBM antenna gain (calculated)	
Beacon	Total receiver system gain:	40.4 dB	
transmitter	-Average RF receiver gain	-4.7 dB	
	Balance(Receiving antenna gain)	35.7 dB	35.7 dB
Radar	E.I.R.P.:	75.8 dBm	
receiver	-Transmitting power	-40.0 dBm	
	Balance(Transmitting antenna gain)	35.8 dB	35.9 dB
Transponder	Overall radar system gain :	116.6 dB	

Then, the receiving antenna gain of the active array is given as

$$G_r = (4\pi/\lambda^2)nA_eW. (6)$$

In the measurement, the total receiver system gain $(4\pi/\lambda^2)nA_e|g|^2W$ (antenna gain + RF receiver gain in decibels) is obtained from the measured $P_{\rm out}$ under given S. The average RF receiver gain $|g|^2$ is obtained by averaging the RF receiver gain of each array element. Then, the antenna gain is derived and is compared with that calculated from the element gain and the amplitude distribution. Good coincidence is obtained between the two values as shown in the second row in Table II. In the on-orbit calibration of TRMM-PR, $|g|^2$ will be obtained from the satellite house-keeping telemetry.

In the ARC measurement of the radar receiver, the received signal level at the ARC gives the *E.I.R.P.* of the PR-BBM, and the results are listed in the third row in Table II. Because the transmission power is measured at the feed point of each element, the transmission antenna gain of PR-BBM is obtained in this case. Excellent coincidence is again obtained between the measurement and the calculation. It should be noted that the reception and transmission antenna gain is not exactly the same in active arrays. In the transponder measurement, the overall radar system gain is obtained at once and shows good consistency between the sum of the results obtained in the previous two one-way measurements. This round-trip measurement assures the reliability of the ARC measurements.

IV. CONCLUSION

An ARC was developed for the on-orbit calibration of the Precipitation Radar (PR) onboard the TRMM satellite. In addition to the delayed-transponder measurement, one-way measurements of the beacon transmitter and the radar receiver are useful in diagnosing the individual performance of the TRMM-PR's receiver and transmitter. A ground-based measurement using a prototype ARC and a breadboard model of the TRMM-PR was conducted to demonstrate the capability of the TRMM-PR calibration. The time-delay function in the transponder proved effective for separating the signal from the clutter echo in the measurement. Excellent coincidence in the antenna gain of PR-BBM was obtained between the ARC measurement and the calculation. The results from three types of the ARC measurement are highly consistent, which suggests the accuracy and reliability of the measurement. Although the results obtained in the shortterm measurements conducted so far using the prototype ARC and the current experimental setup are shown in the present paper, measurements over a long-term are needed to assess the stability of the ARC calibration prior to the actual satellite operation.

ACKNOWLEDGMENT

The authors express special thanks to the TRMM group in the Earth Observation Satellite Department of the National Space Development Agency of Japan for useful discussion and advice. The ARC and the antenna of PR-BBM were manufactured by TOSHIBA. The transmitter and the receiver system of the PR-BBM was manufactured by NEC.

REFERENCES

- D. R. Brunfeldt and F. T. Ulaby, "Active reflector for radar calibration," IEEE Trans. Geosci. Remote Sensing, vol. GE-22, pp. 165–169, 1984.
- [2] M. Fujita, "An active reflector for SAR calibration having a frequency shift capability," *IEICE Trans. Commun.*, vol. E75-B, pp. 791-793, 1992.
- [3] J. Simpson, R. Adler, and G. North, "A proposed Tropical Rainfall Measuring Mission (TRMM) satellite," *Bull. Amer. Meteor. Soc.*, vol. 69, pp. 278–295, 1988.
- [4] T. Kawanishi, H. Takamatsu, T. Kozu, K. Okamoto, and H. Kumagai, "TRMM Precipitation Radar," in *Proc. IGARSS*, Tokyo, 1993, pp. 423–425.
- [5] H. Kumagai, K. Okamoto, T. Kozu, and T. Ihara, "Development of an eight-element-model for TRMM precipitation radar," in *Proc. Microwave Instrumentation for Remote Sensing of the Earth, SPIE*, Orlando, FL, 1993, vol. 1935, pp. 12–16.
- [6] J. J. Lee, "G/T and noise figure of active array antennas," IEEE Trans. Antennas Propagat., vol. AP-41, pp. 241-244, 1984.

An Extension of the Jeffreys-Matusita Distance to Multiclass Cases for Feature Selection

Lorenzo Bruzzone, Fabio Roli, and Sebastiano B. Serpico

Abstract—The problem of extending the Jeffreys-Matusita distance to multiclass cases for feature-selection purposes is addressed and a solution equivalent to the Bhattacharyya bound is presented. This extension is compared with the widely used weighted average Jeffreys-Matusita distance both by examining the respective formulae and by experimenting on an optical remote-sensing data set.

I. Introduction

In remote-sensing image classification, many features (e.g., vegetation indices, texture features) can be computed from commonly available multispectral images in order to characterize data classes of interest to the user. Unfortunately, in practical situations involving a limited number of training samples, addition of features may even degrade classification accuracy (this effect is referred to as the Hughes phenomenon) [1], [2]. Moreover, the computational cost

Manuscript received April 11, 1995; revised July 25, 1995. This work was carried out within the framework of the cooperative research project MEDALUS II (Mediterranean Desertification and Land Use), which was supported by the EEC under the Environment Programme under Contract CT-EV-5V-0166.

The authors are with the Department of Biophysical and Electronic Engineering, University of Genoa, I-16145 Genova, Italy.

IEEE Log Number 9415597.

of classification increases with the number of features used [3]. Therefore, various "feature selection" techniques have been proposed in the pattern recognition literature to reduce the number of features. Among the most widely used, there are the techniques based on "statistical separability indices," which allow one to select a suitable subset of features by assessing the degree of interclass separability associated with each subset considered [3]. In particular, the index based on the Jeffreys–Matusita (J–M) distance has been reported by many authors to be an appropriate measure for feature selection (see, for instance, [3] and [4]).

The J-M index is a pairwise distance measure that can be naturally applied to two-class cases. Various extensions have been proposed in the literature to use such distance when dealing with more than two classes [3].

In this paper, we present an extension of the J-M distance to multiclass cases that, from the viewpoint of feature selection, is equivalent to the Bhattacharyya bound [2], [6] (Section II). This extension is compared with the widely used weighted average J-M distance both by examining the respective formulae (Section II) and by experimenting on an optical remote-sensing data set (Section III).

II. EXTENDING THE JEFFREYS-MATUSITA DISTANCE TO MULTICLASS CASES

In the literature, the J-M distance has been defined as follows [3], [7]:

$$J_{ij} = \left\{ \int_{\mathbf{x}} \left[\sqrt{p(\mathbf{x}/\omega_i)} - \sqrt{p(\mathbf{x}/\omega_j)} \right]^2 d\mathbf{x} \right\}^{1/2}$$
 (1)

where $p(\mathbf{x}/\omega_i)$ and $p(\mathbf{x}/\omega_j)$ are the conditional probability density functions for the feature vector \mathbf{x} , given the data classes ω_i and ω_j , respectively. Equation (1) can be also rewritten as [3], [8]

$$J_{ij} = \sqrt{2(1 - e^{-b_{ij}})} \tag{2}$$

where b_{ij} is the Bhattacharyya distance, defined as [2]

$$b_{ij} = -\ln\left\{ \int_{-\pi} \sqrt{p(\mathbf{x}/\omega_i)p(\mathbf{x}/\omega_j)} d\mathbf{x} \right\}. \tag{3}$$

As has been pointed out in Section I, the J-M index is a measure of statistical separability for two-class cases. Various strategies have been devised to extend it to multiclass cases. The most common lies in using the average J-M distance, computed over all pairs of classes as [3]

$$J_{\text{ave}} = \sum_{i=1}^{C} \sum_{j=1}^{C} p(\omega_i) p(\omega_j) J_{ij}$$
 (4)

where "C" is the number of data classes considered, $p(\omega_i)$ and $p(\omega_j)$ are the *a priori* class probabilities, and J_{ij} is defined according to (1).¹

Another strategy is to select the feature subset that allows the best separation between the least separable pair of classes [3].

In the following, we show a different extension of the J-M distance that, from the viewpoint of feature selection, is equivalent to the Bhattacharyya bound for multiclass cases.

When more than two classes are present, an upper bound to the Bayes error P_e is provided by a combination of the pairwise

¹It is worth noting that (4) can be rewritten as

$$J_{\text{ave}} = 2\sum_{i=1}^{C} \sum_{j>i}^{C} p(\omega_i) p(\omega_j) J_{ij}$$

as $J_{ij} = J_{ji}$ and $J_{ij} = 0$ if i = j.

Bhattacharyya bounds, computed over all pairs of classes as [2], [6],

$$P_e \le \sum_{i=1}^C \sum_{i>j}^C \sqrt{p(\omega_i)p(\omega_j)} e^{-b_{ij}}.$$
 (5)

By using (2), we can rewrite the above upper bound as a function of the pairwise J-M distances

$$P_{e} \leq \sum_{i=1}^{C} \sum_{j>i}^{C} \sqrt{p(\omega_{i})p(\omega_{j})} - \frac{1}{2} \sum_{i=1}^{C} \sum_{j>i}^{C} \sqrt{p(\omega_{i})p(\omega_{j})} J_{ij}^{2}.$$
 (6)

Such an upper bound can be minimized by maximizing the term containing the J-M distances. Therefore, a possible extension of the J-M distance to multiclass cases is given by

$$J_{\rm Bh} = \sum_{i=1}^{C} \sum_{j>i}^{C} \sqrt{p(\omega_i)p(\omega_j)} J_{ij}^2 \tag{7}$$

where the subscript Bh is used to recall that the extension is equivalent to the Bhattacharyya bound.²

For two-class cases, it is easy to verify that the maximization of the J-M distance (see (1)) is equivalent to the minimization of the Bhattacharyya bound. The extension maintains such equivalence also for multiclass cases (while this does not hold true for the average J-M distance). Although it cannot be proved that $J_{\rm Bh}$ always performs better than J_{ave} in selecting features, a comparison between (4) and (7) can point out an interesting aspect of the proposed extension. The two extensions "weight" in different ways the terms containing the J-M distances. In particular, $J_{\rm Bh}$ weights the term containing the J-M distances between couple of classes with the square root of the product of the related a priori probabilities while J_{ave} utilizes the product of the a priori probabilities. It is easy to conclude that the relative importance of data classes with low probabilities of occurrence increases in the presented extension. This can be an advantage in applications with very different a priori probabilities when high classification errors are not acceptable neither for low probability classes.

III. EXPERIMENTAL RESULTS

A. Data Set Description

The considered data set refers to an agricultural area near the village of Feltwell (UK). We selected a section of a scene acquired with a Daedalus 1268 Airborne Thematic Mapper (ATM) scanner. The flight took place in July 1989. The ground truth was used to prepare a thematic map of the selected section; such a map was utilized as a reference map to evaluate the classification accuracy. For our experiments, we considered five agricultural classes (i.e., wheat, sugar beets, potatoes, carrots, and stubble). The data-set pixels were obtained by subsampling the related fields.

To form a "feature vector" for each pixel, we selected the six ATM channels corresponding to Thematic Mapper (TM) channels in the visible and in the infrared spectrum (the thermal band was disregarded). This choice was made to simulate commonly used TM data [10].

B. Results

The Bayesian classifier with multivariate normal distributions was used as a decision rule to assess the classification accuracy provided by each selected feature set. In particular, the proposed extension

 2 It is worth noting that the term J_{ij}^2 is a distance measure that occurs in the work of Jeffreys [10].

78.46

93.42

96.33

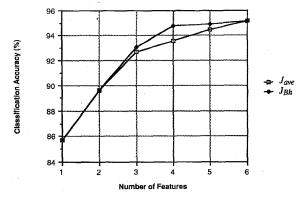
92.78

Average J-M Distance (J_{ave}) for the Selection of the Best Four-Channel Combination					
Data Class	Number of Pixels	A Priori Probability	Jave Classification Accuracy (%)	J _{Bh} Classification Accuracy (%)	
Wheat	353	0.20	95.18	99.15	
Sugar Reets	728	0.41	94 23	95.05	

0.11

0.10

TABLE I COMPARISON BETWEEN THE EXTENSION EQUIVALENT TO THE BHATTACHARYYA BOUND $(J_{\rm Bh})$ and the Average J–M Distance $(J_{\rm ave})$ for the Selection of the Best Four-Channel Combination



Potatoes

Carrots

Stubble

Overall Accuracy

195

319

191

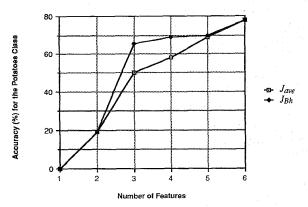
Fig. 1. Comparison between the extension equivalent to the Bhattacharyya bound $(J_{\rm Bh})$ and the average J–M distance $(J_{\rm ave})$. The classes considered and the related numbers of pixels are given in Table II.

(see (7)) was compared with the average J–M distance (see (4)). For the described data set, $J_{\rm Bh}$ performed better in selecting the best four-channel combination (Table I). As expected, it yielded the best result for a class with a low *a priori* probability (i.e., potatoes). The two considered extensions of the J–M distance provided the same classification accuracy for the other channel combinations.

In order to better assess the advantages of the presented extension for classes with low *a priori* probabilities, we simulated a new data set, reducing the probabilities of occurrence for the wheat and potatoes classes (Table II). This was accomplished by further subsampling such classes. In this experiment, $J_{\rm Bh}$ provided the overall classification accuracy given in Fig. 1. It performed better than $J_{\rm ave}$ in selecting various channel combinations. In particular, a sharp increase in classification accuracy was obtained for the potatoes class, which had a low probability of occurrence (Fig. 2).

IV. CONCLUSION

In this paper, we have addressed the problem of extending the J-M distance to multiclass cases for feature selection purposes. We have presented an extension which, differently from the commonly used average J-M distance, maintains a property of the pairwise J-M distance, that is, its maximization is equivalent to the minimization of the Bhattacharyya bound of the error probability. In addition, as compared with the average J-M distance, it gives greater importance to data classes with low *a priori* probabilities in the selection process. This behavior can be particularly useful for classification tasks, when classes with very different *a priori* probabilities are present. This advantage was confirmed by the reported experiments, as the presented extension performed better than the average J-M distance, in particular, for data classes with low *a priori* probabilities.



85.64

94.67

96.86

94.96

Fig. 2. Comparison between the extension equivalent to the Bhattacharyya bound $(J_{\rm Bh})$ and the average J-M distance $(J_{\rm ave})$ for the potatoes class. The classes considered and the related numbers of pixels are given in Table II.

TABLE II
THE CLASSES CONSIDERED AND THE RELATED NUMBERS OF PIXELS OBTAINED BY REDUCING THE A PRIORI PROBABILITIES FOR THE WHEAT AND POTATOES CLASSES

Data Class	Number of Pixels	A Priori Probability 0.06	
Wheat	90		
Sugar Beets	728	0.51	
Potatoes	90	0.06	
Carrots	319	0.23	
Stubble	191	0.14	

From a feature selection viewpoint, the presented extension performs as well as the Bhattacharyya bound. However, we think that the fact that the presented extension is explicitly formulated in terms of pairwise J–M distances makes clearer for the remote-sensing community the difference between the Bhattacharyya bound and the commonly used average J–M distance. Finally, it is worth noting that the presented extension, the average J–M distance, and the criterion based on the least separable pairs of classes can be implemented by a single computer program, as all of them are computed from *a priori* class probabilities and pairwise J–M distances.

ACKNOWLEDGMENT

The authors are grateful to the anonymous referees for their constructive criticisms.

REFERENCES

 B. Kim and D. A. Landgrebe, "Hierarchical classifier design in highdimensional, numerous class cases," *IEEE Trans. Geosci. Remote Sens*ing, vol. 29, no. 4, pp. 518–528, July 1991.

- [2] K. Fukunaga, Introduction to Statistical Pattern Recognition, 2nd ed. New York: Academic, 1990.
- [3] P. H. Swain and S. M. Davis, Remote Sensing: The Quantitative Approach. New York: McGraw-Hill, 1978.
- [4] I. L. Thomas, N. P. Ching, V. M. Benning, and J. A. D'Aguanno, "A review of multi-channel indices of class separability," Int. J. Remote Sensing, vol. 8, no. 3, pp. 331-350, 1987.
- [5] D. G. Lainiotis, "A class of upper bounds on probability of error for multihypotheses pattern recognition," IEEE Trans. Inform. Theory, vol. IT-15, pp. 730-731, Nov. 1963.
- A. G. Wacker, "Minimum distance approach to classification," Ph.D. dissertation, Lab. Applicat. Remote Sensing, School Elect. Eng., Purdue Univ., West Lafayette, IN, 1971.
- G. T. Toussaint, "Some inequalities between distance measure for feature evaluation," IEEE Trans. Comput., vol. C-21, no. 4, pp. 409-410, Apr.
- [8] S. J. Whitsitt and D. A. Landgrebe, "Error estimation and separability measure in feature selection for multiclass pattern recognition," School Elect. Eng., Purdue Univ., West Lafayette, IN, Tech. Rep. 77-34, 1977.
- H. Jeffreys, Theory of Probability. New York: Oxford Univ. Press,
- [10] J. R. G. Townshend, "Agricultural land-cover discrimination using thematic mapper spectral bands," Int. J. Remote Sensing, vol. 5, pp. 681-698, 1984.

Infrared Extinction of the Powder of Brass 70Cu/30Zn Calculated by the FDTD and Turning Bands Methods

Hsing-Yi Chen, I.-Young Tarn, and Yeou-Jou Hwang

Abstract-The finite-difference time-domain (FDTD) method is used to calculate the specific extinction cross section of the powder of brass 70Cu/30Zn with 10^3 to 2.16×10^5 cubical particles for cell sizes in the range of 0.025 to 0.5 μm at infrared frequency. The digitized models with a random process using the turning bands method are simulated for the powder of brass 70Cu/30Zn. From theoretical calculations, the value of specific extinction cross section of the powder of brass 70Cu/30Zn is between 0.1 to 4.6 m²/g. While from the experimental measurement, the value of specific extinction cross section is between 0.58 to 3.78 m²/g. Most of the theoretical results make a good agreement with those obtained from the experimental measurements for the cell sizes of particles in the range of 0.025 to 0.5 μ m. From the numerical calculations, it is also found that there is a resonant extinction value occurred at the resonant particle size d_0 which is approximately $2.54 \times n_p^{-0.293}$ μm determined by a least square curve fitting method, where n_p is the number of particles. The resonant value calculated by the numerical solution is larger than the maximum value obtained from the experimental measurement.

I. INTRODUCTION

One of the military applications of electromagnetic absorption and scattering of the powder of brass 70Cu/30Zn (70% of Cu and 30% of Zn) [1] is the tank detection avoidance technique. Tanks must be provided with the best means of protection. Visual and Infrared screening smoke (VIRSS) grenades have been developed for the tank survivability by the Royal Ordnance in the UK [2].

There are several analytical methods suitable for calculating the electromagnetic scattering and absorption by particle objects [3]-[8].

Manuscript received September 19, 1994; revised July 21, 1995. This work was supported by the National Science Council of the Republic of China under Grant NSC 82-0404-E-155-002.

The authors are with the Department of Electrical Engineering, Yuan-Ze Institute of Technology, Taoyuan Shian, Taiwan 32026 R.O.C.

IEEE Log Number 9415598.

Among them, a better approach is the Iskander-Chen-Penner solution (I-C-P) [8], which uses a volume integral equation formulation (VIEF) together with the method of moments (MOM). However, the I-C-P solution proposed in the previous works for particles over one thousand has been hindered by computer resources.

Recently, the Finite-Difference Time-Domain (FDTD) method has become increasingly popular for computations of electromagnetic wave propagation and scattering problems [9]-[11]. In this paper, the FDTD method is used to solve the Maxwell's equations for electric and magnetic fields induced in the powder of brass 70Cu/30Zn. On the other hand, the turning bands method [12] is used to generate the digitized models through a random process. The number of particles used in the calculations is in the range of 10^3 to 2.16×10^5 . The refractive index of the powder of brass 70Cu/30Zn is taken to be $n^* = 16.87 + j 51.59$ at wavelength $\lambda = 10 \mu m$ [1]. The cell sizes of these cubical particles are varied from 0.025 to 0.5 μ m to examine the extinction characteristic. Results of the extinction cross section are presented and compared with the experimental data at infrared frequency (wavelength $\lambda = 10 \mu \text{m}$).

II. THE FDTD METHOD

The FDTD method, first presented by Yee [13] in 1966 and later developed by many researchers [14]-[17], is based on direct solution of Maxwell's time-dependent curl equations

$$\nabla \times \bar{E} = -\mu \frac{\partial \bar{H}}{\partial t} \tag{1}$$

$$\nabla \times \bar{E} = -\mu \frac{\partial \bar{H}}{\partial t}$$

$$\nabla \times \bar{H} = \sigma \bar{E} + \varepsilon \frac{\partial \bar{E}}{\partial t}.$$
(1)

The components of EM fields \bar{E} and \bar{H} are positioned at halfstep interval around a unit cell. σ , μ , and ε are the conductivity, permeability, and permittivity of the objects, respectively. In the FDTD method, the coupled Maxwell's equations in the differential form are solved for various points of the scatters as well as its surroundings in a time-stepped manner until converged solutions are obtained.

It should be noted that the FDTD method divides the computation space into total-field zone and scattered-field zone as shown in Fig. 1. The total-field zone encloses the scattering particles and the scatteredfield zone is chosen to numerically mimic the unbounded region outside the total-field region by absorbing the outgoing scattered waves. Another important problem encountered in solving the timedomain electromagnetic-field equation, using the FDTD method, is the absorbing boundary conditions. In our formulation, the secondorder approximation of absorbing boundary conditions [16] is used to limit the computational domain by simulating unbounded space. In the simulations, the cell sizes are taken to be a fraction (<1/20) of the wavelength in order to accurately obtain the numerical results. To ensure stability, the time increment δ_t is given by $\delta/2C_0$ [17], where C_0 is the speed of light in free space and δ is the cell size.

III. THE TURNING BANDS METHOD

It is possible to use the turning bands method [12], [18] to generate discrete samples of the random process for a stationary and isotropic random medium. Let the random process function η and the correlation function N are used in the study for random particles located in the 3-D space. According to the turning bands method, any 3-D simulation can be reduced to several independent